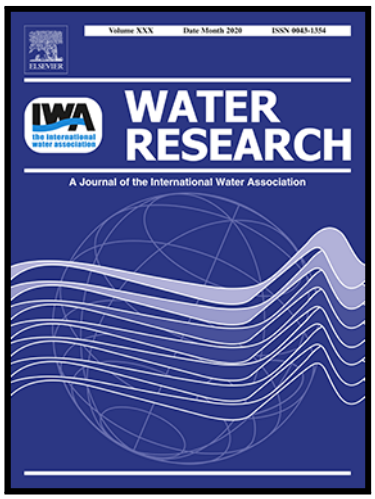

nEfficiency of pre-oxidation of natural organic matter for the mitigation of disinfection byproducts: Electron Donating Capacity and UV absorbance as surrogate parameters

Valentin Rougé , Urs von Gunten , Sébastien Allard

PII: S0043-1354(20)30953-2
DOI: https://doi.org/10.1016/j.watres.2020.116418
Reference: WR 116418

To appear in: *Water Research*

Received date: 17 June 2020
Revised date: 8 September 2020
Accepted date: 9 September 2020

Please cite this article as: Valentin Rougé , Urs von Gunten , Sébastien Allard , nEfficiency of pre-oxidation of natural organic matter for the mitigation of disinfection byproducts: Electron Donating Capacity and UV absorbance as surrogate parameters, *Water Research* (2020), doi: https://doi.org/10.1016/j.watres.2020.116418

Highlights

- Chemical oxidation abates the electron donating capacity (EDC) more efficiently than UV_{254}.
- The efficiency on UV_{254} abatement ranked O_3 > Mn(VII) > Fe(VI)/ClO_2
- The efficiency on EDC abatement ranked Mn(VII) > ClO_2 > Fe(VI) > O_3
- Good correlation between EDC abatement and haloacetonitrile mitigation

Efficiency of pre-oxidation of natural organic matter for the mitigation of disinfection byproducts: Electron Donating Capacity and UV absorbance as surrogate parameters

Valentin Rougé,[†,§] *Urs von Gunten,**[‖,‡,⊥] *Sébastien Allard**[,†]

[†]Curtin Water Quality Research Centre, Department of Chemistry, Curtin University, GPO Box U1987, 6845 Perth, Western Australia, Australia

[§]School of Earth Sciences and Environmental Engineering, Gwangju Institute of Science and Technology (GIST), Gwangju 61005, Republic of Korea

[‖]Eawag, Swiss Federal Institute of Aquatic Science and Technology, CH-8600 Dübendorf, Switzerland

[‡]School of Architecture, Civil and Environmental Engineering (ENAC), Ecole Polytechnique Fédérale Lausanne (EPFL), CH-1015 Lausanne, Switzerland

[⊥]ETH Zurich, Swiss Federal Institute of Technology, Institute of Biogeochemistry and Pollutant Dynamics (IBP), Department of Environment Systems (D-USYS), Universitätstrasse 16, CH-8092 Zürich

*Corresponding authors: (S.A.) phone: +61 8 9266 7949; e-mail: s.allard@curtin.edu.au. (U.v.G.) phone: +41 58 765 5270; e-mail: urs.vongunten@eawag.ch.

Abstract

Pre-oxidation is often used before disinfection with chlorine to decrease the reactivity of the water matrix and mitigate the formation of regulated disinfection byproducts (DBPs). This study provides insights on the impact of oxidative pre-treatment with chlorine dioxide (ClO_2), ozone (O_3), ferrate (Fe(VI)) and permanganate (Mn(VII)) on Suwannee River Natural Organic Matter (SRNOM) properties characterized by the UV absorbance at 254 nm (UV_{254}) and the electron donating capacity (EDC). Changes in NOM reactivity and abatement of DBP precursors are also assessed. The impact of pre-oxidants (based on molar concentration) on UV_{254} abatement ranked in the order O_3 > Mn(VII) > Fe(VI)/ClO_2, while the efficiency of pre-oxidation on EDC abatement followed the order Mn(VII) > ClO_2 > Fe(VI) > O_3 and two phases were observed. At low specific ClO_2, Fe(VI) and Mn(VII) doses corresponding to < 50% EDC abatement, a limited relative abatement of UV_{254} compared to the EDC was observed (~ 8% EDC abatement per 1% UV_{254} abatement). This suggests the oxidation of phenolic-type moieties to quinone-type moieties which absorb UV_{254} and don't contribute to EDC. At higher oxidant doses (> 50% EDC abatement), a similar abatement of EDC and UV_{254} (~ 0.9–1.2% EDC abatement per 1% UV_{254} abatement) suggested aromatic ring cleavage. In comparison to the other oxidants, O_3 abated the relative UV_{254} more effectively, due to a more efficient cleavage of aromatic rings. For a pre-oxidation with Mn(VII), ClO_2 and Fe(VI), similar correlations between the EDC abatement and the chlorine demand or the adsorbable organic halide (AOX) formation were obtained. In contrast, O_3 pre-treatment led to a lower chlorine demand and AOX formation for equivalent EDC abatement. For all oxidants, trihalomethane formation was poorly correlated with both EDC and UV_{254}. The EDC abatement was found to be a pre-oxidant-independent surrogate for haloacetonitrile formation. These results emphasize the benefits of combining EDC and UV_{254} measurement to understand and monitor oxidant-induced changes of NOM and assessing DBP formation.

Keywords: Electron donating capacity (EDC), chemical pre-oxidation, natural organic matter (NOM), disinfection byproduct (DBP), UV absorbance (UV254); chlorine disinfection

1. Introduction

During water treatment, a large fraction of chlorine (Free Available Chlorine, FAC), the most commonly used disinfectant, reacts with natural organic matter (NOM), partially leading to the formation of disinfection byproducts (DBPs) (Richardson et al. 2007, Sedlak and von Gunten 2011, von Gunten 2018). Pre-oxidation is a possible treatment option to reduce NOM reactivity towards chlorine prior to disinfection and to mitigate DBP formation (Gallard and von Gunten 2002, Gan et al. 2015, Yang et al. 2013b). Depending on the type of oxidant, the water characteristics and the type of DBPs, differences in DBP mitigation efficiency have been observed during pre-oxidation treatment (de Vera et al. 2015, Gan et al. 2015, Jiang et al. 2016c, Yang et al. 2013a, Yang et al. 2013b). In previous studies, the efficiency of oxidants has been compared based on their concentrations/doses (Jiang et al. 2016b, Xie et al. 2013). In other studies, virus inactivation efficiency (Selbes et al. 2014), or the concentration of oxidants commonly used in drinking water plants guided the choice of their doses (Jones et al. 2012, Xie et al. 2013, Yang et al. 2013b). However, each oxidant used for pre-oxidation has its own characteristics. Chlorine dioxide (ClO_2) reacts with NOM moieties (e.g., activated aromatic moieties) through a one-electron transfer to form chlorite (ClO_2^-). Recent studies have also highlighted the importance of oxygen transfer mechanisms releasing FAC (Rougé et al. 2018, Terhalle et al. 2018). FAC released by ClO_2 can then react through a two-electron oxidation or electrophilic aromatic substitution (Criquet et al. 2015). Ozone (O_3) is particularly reactive towards olefins, leading to cleavage of C=C bonds through the Criegee mechanism, activated aromatic moieties, or neutral amines (Lim et al. 2019, von Sonntag and

von Gunten 2012). O_3 reacts mostly by oxygen or electron transfer associated with the possible release of hydroxyl radical ($^{\bullet}OH$), singlet oxygen ($^1O_2$), superoxide radical ($O_2^{\bullet-}$) or hydrogen peroxide (H_2O_2) (von Gunten 2003). $^{\bullet}OH$ released by O_3 exhibits a very high reactivity towards a wide range of moieties, mostly through addition or hydrogen abstraction (von Sonntag 2007). Permanganate (Mn(VII)) and ferrate (Fe(VI)) can react through electrophilic attack on double bonds (olefins), or electron transfer, notably with phenolic compounds and neutral amines (Perez-Benito 2009, Shin and Lee 2016, Waldemer and Tratnyek 2006). Furthermore, the products of these oxidants, Mn(VI), Mn(V) and Fe(V) , are also highly reactive (Rush and Bielski 1995, Rush et al. 1995, Simándi and Záhonyi-Budó 1998, Záhonyi-Budó and Simándi 1996).

Considering the large array of reaction mechanisms, it is difficult to compare the impact of each pre-oxidation treatment on the mitigation of DBPs based on a specific oxidant dose. Comparing the reactivity of oxidants based on their impact on NOM characteristics may be an interesting alternative. The absorbance at 254 nm (UV_{254}), or the $SUVA_{254}$ (UV absorbance at 254 nm divided by the concentration of the dissolved organic carbon, DOC), have been widely used as proxies for NOM aromaticity and its reactivity towards chlorine (Croué et al. 2000, Reckhow et al. 1990, Weishaar et al. 2003). The capacity of other spectrophotometric indicators, e.g., the absorbance at 272 nm or spectral slopes, to characterize organic matter has also been investigated (Helms et al. 2008, Korshin et al. 1997b, Wenk et al. 2013). These spectrophotometric indicators were shown to correlate with the formation of DBPs such as trihalomethanes (THMs), haloacetic acids or adsorbable organic halogen (AOX) in some studies (Amy et al. 1987, Archer and Singer 2006, Chen and Valentine 2008, Croué et al. 2000, Edzwald et al. 1985, Korshin et al. 1996, 1997a, Korshin et al. 2002). However, poor correlations between $SUVA_{254}$ or UV_{254} and DBP formation have been reported in other investigations (Ates et al. 2007, Weishaar et al. 2003). Recently, the

measurement of the electron donating capacity (EDC) was developed, based on a one-electron transfer from NOM to a radical, $ABTS^{+\bullet}$ (2,2'-azino-bis(3-ethylbenzothiazoline-6-sulfonic acid) (Aeschbacher et al. 2012, Önnby et al. 2018b). Monitoring the $ABTS^{+\bullet}$, either by spectrophotometry or chronoamperometry (Chon et al. 2015, Walpen et al. 2016), allows for the estimation of the electrons availability in DOM for its reactions with oxidants. This method has been successfully applied to characterize the DOM reactivity with oxidants (de Vera et al. 2017, Önnby et al. 2018a, Remucal et al. 2020, Walpen et al. 2020), and used as a proxy for activated aromatic moieties in NOM (Aeschbacher et al. 2012, Walpen et al. 2016), which are important precursors of halogenated DBPs. Furthermore, the use of EDC combined with UV_{254} allowed to better understand the reaction mechanisms of ClO_2, O_3 and FAC with NOM (Önnby et al. 2018a, Wenk et al. 2013). Notably, the oxidation of phenolic-type moieties to quinone-type moieties leads to a higher EDC abatement (quinone-type moieties are poor electron-donating compounds) compared to the UV_{254} abatement (quinone-type moieties retain some absorbance). It has been demonstrated that ClO_2 oxidation leads to a limited EDC abatement compared to UV_{254}, which was explained by the formation of quinone-type moieties (Wenk et al. 2013). In comparison to ClO_2, O_3 abated more UV_{254} due to, in part, the opening of aromatic rings (Wenk et al. 2013). However, at near neutral pH (in presence of an $^{\bullet}OH$ quencher) the relative abatement of EDC was still more pronounced than for UV_{254}, suggesting that quinone-type moieties were also formed with O_3 under these conditions (Önnby et al. 2018a).

The aims of this study are (i) to compare the impact of increasing doses of ClO_2, O_3, Fe(VI) and Mn(VII) on NOM properties, i.e. EDC and UV_{254} abatement, based on their known reaction mechanisms with model compounds and (ii) to explore the possibility of using the EDC and UV_{254} as complementary pre-oxidant-independent surrogates for predicting the chlorine demand and the formation of DBP during post-disinfection. The impact of different

pre-oxidant doses of ClO_2, O_3, Fe(VI) and Mn(VII) on Suwannee River NOM (SRNOM) extract characteristics was monitored using both the EDC and UV_{254}. The pre-oxidized samples were then chlorinated and the chlorine consumption, the AOX, THM and haloacetonitrile (HAN) formation were compared to the measured NOM extract characteristics (EDC and UV_{254}).

2. Materials and methods

2.1. Chemicals and reagents.

Sodium chlorite (80%) and a sodium hypochlorite solution (10–15%) were purchased from Sigma-Aldrich, with impurities being mostly chloride and traces of chlorate (< 0.01 µM of ClO_3^- per µM of NaOCl or $NaClO_2$). All other chemicals were of analytical grade quality (≥ 98%). Solutions were prepared with ultrapure water (Purelab Ultra, Elga, UK). SRNOM extract was purchased from the International Humic Substances Society (Cat. No. 2R101N).

2.2. Preparation of oxidant solutions.

Chlorine stock solutions were prepared from a sodium hypochlorite solution standardized by direct UV measurement at 292 nm (ε_{292} = 362 M^{-1} cm^{-1}) (Furman and Margerum 1998). ClO_2 was produced by mixing solutions of sodium persulfate (40 g L^{-1}) and sodium chlorite (80 g L^{-1}) under N_2 bubbling for about 1 h (Gates 1998, Granstrom and Lee 1958). The ClO_2 was retrieved in chilled ultrapure water and standardized by direct UV measurement at 359 nm (ε_{359} = 1230 M^{-1} cm^{-1}) (Furman and Margerum 1998). K_2FeO_4 was prepared by oxidation of 0.186 mol of ferric nitrate nonahydrate with 0.845 mol of potassium hypochlorite in a concentrated potassium hydroxide solution (Li et al. 2005). The final solid product was stable with a purity of 43%, the rest of the solid being potassium hydroxide or potassium chloride. Mn(VII) and Fe(VI) solutions were prepared by dissolution of $KMnO_4$ in ultrapure water for Mn(VII), or of K_2FeO_4 in a phosphate/borate buffer (5 mM/1 mM, pH

9.5) for Fe(VI). The stock solutions (1–5 mM) were then filtered through 0.22 µm (polyethersulfone, Merck Millipore) and standardized by direct UV measurement at 525 nm (ε_{525} = 2430 M^{-1} cm^{-1}) (Ramseier et al. 2011) for Mn(VII) or 510 nm (ε_{510} = 1150 M^{-1} cm^{-1}) (Lee et al. 2005b) for Fe(VI). O_3 stock solutions were prepared by bubbling an ozone-oxygen mixture produced by an O_3 generator (American Ozone System Inc.) in ultrapure water cooled at < 5°C. The O_3 stock solution (0.6–0.9 mM) was standardized by direct UV measurement at 260 nm (ε_{260} = 3200 M^{-1} cm^{-1}) (von Sonntag and von Gunten 2012).

2.3. Pre-oxidation and chlorination experiments.

Synthetic waters were prepared with 3.0 mgC L^{-1} of a SRNOM extract buffered at pH 8 (40 mM borate), with or without bromide (150 or 500 µg L^{-1}). pH 8 was chosen because of the buffering range of borate to prevent the formation of phosphate complexes notably during Fe(VI) or Mn(VII) oxidation (Jiang et al. 2009, Jiang et al. 2016a). For EDC and UV_{254} experiments, 40 mL samples were spiked with O_3 (with or without 5 mM *tert*-butanol, *t*-BuOH), ClO_2, Mn(VII) or Fe(VI) (1–133 µM), vigorously mixed for 10 seconds, kept with negligible headspace (< 10% of total volume) and protected from light until complete depletion of the oxidants. The reaction times ranged from a few seconds to several hours depending on the oxidant and dose. *t*-BuOH was used as a $^{\bullet}OH$ scavenger to account for direct O_3 reactions only (Staehelin and Hoigné 1985). For higher ranges of O_3 doses (> 20 µM), the significant volume of the O_3 stock solution added was taken into account by concentrating the matrix accordingly. After confirming the absence of the oxidants, the samples were filtered through 0.22 µm (polyethersulfone, Merck Millipore) and analyzed for EDC and UV_{254}. The filtration step between pre-oxidation and disinfection was performed to remove Mn(IV) and Fe(III) particles, hence preventing their interaction with FAC. The filtration was not affecting the EDC or UV_{254} quantification. For chlorination experiments, a similar experimental procedure was used with 500 mL samples. After pre-oxidation, 200 mL

of the filtered pre-oxidized sample was chlorinated with 85 µM sodium hypochlorite (6.0 $mgCl_2\ L^{-1}$) for 3 days, with negligible headspace (< 10% of total volume) and protected from light. Preliminary experiments were carried out to determine the chlorine dose needed to obtain an oxidant residual of about 1.5 $mgCl_2\ L^{-1}$ after 3 days at pH 8 for a sample without bromide and without pre-treatment. The oxidant residual was quenched by sulfite (10% excess) for adsorbable organic halide (AOX) measurements, or by a large excess (4–5 times) of ascorbic acid for THM and HAN measurements.

2.4. Analytical methods.

THMs (trichloromethane, bromodichloromethane, dibromochloromethane, tribromomethane) and HANs (chloroacetonitrile, bromoacetonitrile, dichloroacetonitrile, bromochloroacetonitrile, dibromoacetonitrile, trichloroacetonitrile) were analyzed by headspace GC-MS with a method adapted from previously published studies, of which details are given in the supporting information (SI), Text S1 (Allard et al. 2012, Kristiana et al. 2012). The AOX was measured by combustion and ion chromatography after adsorbing samples on activated carbon (Langsa et al. 2017a). The residual oxidant concentrations were measured by ABTS (Pinkernell et al. 2000, Lee et al. 2005b, Jiang et al. 2012, Wang and Reckhow 2016). The dissolved organic carbon (DOC) concentration of the SRNOM stock solutions was standardized, as non-purgeable organic carbon, using a total organic carbon analyzer from Shimadzu (TOC-L). The EDC and the UV_{254} were measured on an Agilent 1100 series system using a size-exclusion chromatography (SEC), followed by a post-column reaction with an $ABTS^{+\bullet}$ solution for EDC (monitored at 405 nm, see details in Text S2, SI) (Chon et al. 2015, Önnby et al. 2018b). The relative EDC and UV_{254} results are presented as percentage of abatement compared to the untreated sample.

3. Results and discussion

3.1. Impact of oxidation on SRNOM properties.

The relative EDC and UV_{254} abatements (%), were measured after treatment of 3 mgC L^{-1} of SRNOM at pH 8 with different specific doses of ClO_2, O_3 (with or without *t*-BuOH), Fe(VI) or Mn(VII) (Figs. 1a and b). Both the relative EDC and UV_{254} decreased with increasing doses of oxidants and the extent of abatement depended on the type of oxidant.

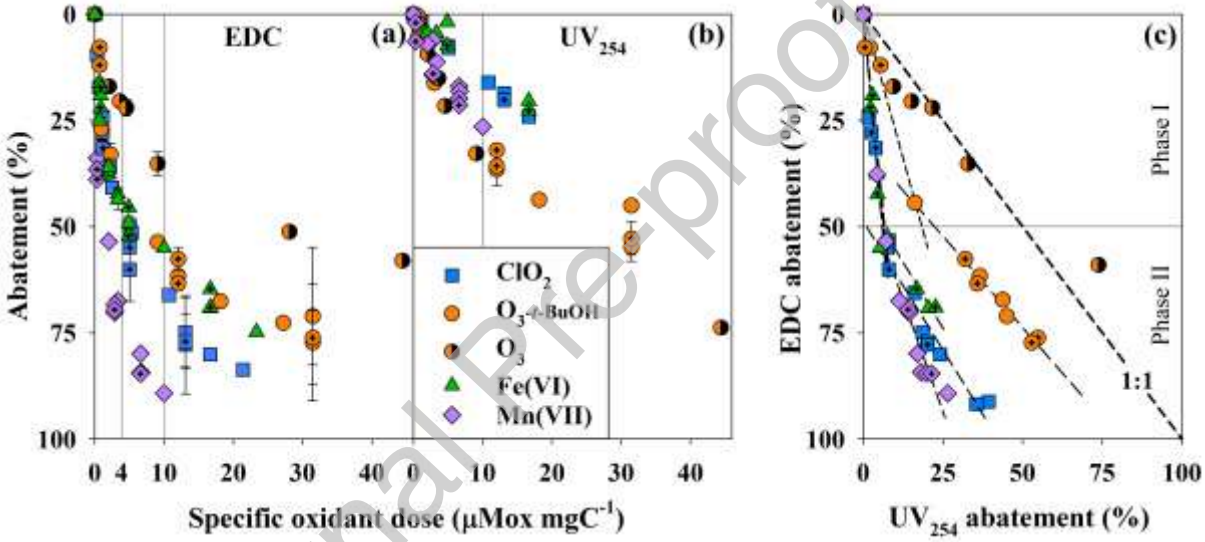

Fig. 1. Relative abatement of (a) EDC and (b) UV_{254} as a function of the specific doses of ClO_2, O_3 (with or without *t*-BuOH), Fe(VI) or Mn(VII) and (c) relationship between EDC and UV_{254} abatement for the selected oxidants. Samples containing bromide are identified by a cross in the symbol. [SRNOM] = 3 mgC L^{-1}, [Br^-] = 0 or 150 µg L^{-1}, pH 8 (40 mM borate), oxidant doses: ClO_2 = 3.3–21.3 µM mgC^{-1}, O_3 in presence of *t*-BuOH (O_3-*t*-BuOH) = 0.7–31.3 µM mgC^{-1} ([*t*-BuOH] = 0.4 mM), O_3 = 2–44.3 µM mgC^{-1}, Fe(VI) = 0.7–23.3 µM mgC^{-1}, Mn(VII) = 0.3–10 µM mgC^{-1}. Error bars represent the range of results of duplicate analyses of a single experiment.

For a specific pre-oxidant dose of 4 µM ox mgC^{-1}, the relative EDC abatement was highest for Mn(VII), with ~ 70–75% EDC abatement, similar for ClO_2, Fe(VI) and O_3 in presence of *t*-BuOH (O_3-*t*-BuOH), with ~ 40–44% EDC abatement, and lowest for O_3 without scavenger (~ 21% EDC abatement) (Fig. 1a). For specific doses > 4 µM ox mgC^{-1}, O_3-*t*-BuOH and Fe(VI) became less efficient than ClO_2 in abating the relative EDC. At 10 µM ox mgC^{-1}, Mn(VII) and ClO_2 abated the EDC by 90 and 65%, respectively, while O_3-*t*-BuOH and Fe(VI) achieved ~ 54% (Fig. 1a). In contrast to the EDC, the relative UV_{254} abatement with O_3 (with and without *t*-BuOH) and Mn(VII) were relatively similar and higher than for ClO_2 or Fe(VI) (Fig. 1b). For a specific pre-oxidant dose of 10 µM ox mgC^{-1}, ~ 30% UV_{254} abatement was achieved by Mn(VII) and O_3 (with and without *t*-BuOH), whereas ClO_2 and Fe(VI) abated the UV_{254} by only 15% (Fig. 1b). To illustrate the differences between oxidants, the relative UV_{254} abatement was plotted against the relative EDC abatement (Fig. 1c). Figs. 1a-c show that O_3 abated the relative EDC and the relative UV_{254} to a similar extent (~ 36% and ~ 34%, respectively, at 10 µM ox mgC^{-1}) while O_3-*t*-BuOH, ClO_2, Fe(VI) and Mn(VII) exhibited much higher relative EDC abatements compared to UV_{254} (> 50% for EDC and ≤ 30% for UV_{254} at 10 µM ox mgC^{-1}). Fig. 1c shows two distinct phases for all four oxidants. In phase I (< 50% EDC abatement), a very limited relative UV_{254} abatement was observed compared to the EDC, whereas in phase II (> 50% EDC abatement), the relative UV_{254} abatement was more pronounced (Fig. 1c). In phase I, the ratio of relative $\Delta EDC/\Delta UV_{254}$ abatement was 3 for O_3-*t*-BuOH and 7–8 for ClO_2, Fe(VI) and Mn(VII) (Table S1, Fig. 1c). In phase II, the relative EDC and UV_{254} abatements were almost equivalent for ClO_2, Fe(VI) and O_3-*t*-BuOH ($\Delta EDC/\Delta UV_{254}$ = 0.9–1.2, Table S1 and Fig. 1c) while Mn(VII) still had a higher relative EDC abatement compared to UV_{254} ($\Delta EDC/\Delta UV_{254}$ ≈ 2). In absence of *t*-BuOH, O_3 featured only one phase (Fig. 1c).

The impact of bromide on the EDC and UV_{254} abatement was also tested. The oxidants exhibit different reactivities with bromide. Among the selected pre-oxidants, O_3 is the most reactive and will oxidize bromide with a moderate rate to free available bromine or even to bromate depending on the ozone exposure, pH and the bromide concentration (von Gunten and Hoigné 1994). Fe(VI) can also oxidize bromide but with a much lower second order rate constant (Jiang et al. 2016a). ClO_2 and Mn(VII) are not reactive towards bromide (Hoigné and Bader 1994, Lawani and Sutter 1973), but ClO_2 can release FAC during reactions with NOM (Rougé et al. 2018), which in turn can oxidize bromide to free available bromine (Kumar and Margerum 1987). The EDC and the UV_{254} abatements were not affected by the addition of bromide (150 and 500 µg L^{-1}, Fig. S1, SI). This suggests that the potential free available bromine formed by O_3 and Fe(VI) had limited impact on the NOM properties, probably due to the efficient reactions of the oxidant-reactive NOM moieties with the primary oxidant. In the case of ClO_2, it can be hypothesized that free available bromine didn't impact NOM characteristics differently than the *in situ* released FAC.

3.2. Mechanistic interpretations.

Activated aromatic moieties such as phenols are considered as major EDC contributors (Aeschbacher et al. 2012). Previous studies showed that ClO_2, O_3, Fe(VI) and Mn(VII) are reacting with such compounds (Lee et al. 2005a, Waldemer and Tratnyek 2006, Tentscher et al. 2018, Hoigné and Bader 1994), which is consistent with the ability of all oxidants to readily abate EDC (Fig. 1a).

3.2.1. EDC and UV_{254} abatement by Mn(VII), Fe(VI) and ClO_2.

As shown in Fig. 1a the relative EDC abatement was higher for Mn(VII) compared to the other oxidants. This is in agreement with the theoretical ability of Mn(VII) to abstract more electrons than the other oxidants (depending on the final oxidation state of Mn, between 3

(reaction to Mn(IV)) and 5 electrons (reaction to Mn(II))). It was verified that the relative EDC abatement by Mn(VII) was not due to the adsorption of NOM onto MnO_2 particles and subsequent filtration of MnO_2 (Allard et al. 2017). The DOC concentration was similar before and after filtration, and a difference ≤ 4% for the EDC abatement was measured between the filtered and unfiltered samples. Similarly to Mn(VII), Fe(VI) is theoretically able to abstract up to 3 (formation of Fe(III)) or 4 electrons (formation of Fe(II)). However, at equivalent specific doses, the EDC abatement for Fe(VI) was much lower than for Mn(VII) (Fig. 1a). Fe(VI) and its reduced products are known to rapidly self-decay (Lee et al. 2014, Rush and Bielski 1989). Therefore, since Fe(VI) exposure is reduced, the EDC abatement is lower than expected. Furthermore, the auto-decomposition of the intermediates Fe(V) and Fe(IV) is likely to be faster than their reaction with NOM moieties (Lee et al. 2014, Rush and Bielski 1995, Rush et al. 1995). In contrast, the much more efficient EDC abatement by Mn(VII) suggests that its reduced products Mn(V) and Mn(VI) are likely to react with NOM moieties. More details on kinetics and degradation pathways of Fe and Mn species are provided in Text S3 (SI). Comparatively to Mn(VII), the lower relative EDC abatement by ClO_2 is consistent with the known one-electron transfer producing ClO_2^- (Fig. 1a) (Gordon et al. 1972), although other mechanisms, notably oxygen transfer which can release FAC (Rougé et al. 2018), coexist and may enhance the oxidation capacity of ClO_2 (discussed in section 3.2.3). The relative EDC and UV_{254} abatements obtained with ClO_2 (Figs. 1a-c) are consistent with a previous study conducted with Suwannee River Fulvic Acid at pH 7 (Wenk et al. 2013).

The generally higher relative EDC abatement compared to UV_{254} abatement was previously explained by the formation of quinones from the oxidation of phenolic moieties, which leads to an abatement of the EDC but not the UV_{254} (quinones also absorb UV light) (Wenk et al. 2013). The relative EDC versus UV_{254} abatements for Mn(VII) and Fe(VI) were similar to

the observations for ClO_2 (Fig. 1c). This suggests that analogous reaction mechanisms may occur with Mn(VII) and Fe(VI), i.e., the formation of quinones. This is consistent with one-electron transfer pathways suggested for the reaction of Mn(VII) and Fe(VI) with phenolic compounds, leading to quinones and/or dimeric structures (Huang et al. 2001, Jiang et al. 2012, Rush et al. 1995, Waldemer and Tratnyek 2006). The presence of two phases for the relative EDC versus UV_{254} plots can provide further insights on the impact of the different oxidants on SRNOM characteristics (Fig. 1c). It is suggested that in phase I (< 50% EDC abatement), ClO_2, Mn(VII) and Fe(VI) oxidized phenolic-type moieties to quinone-type moieties, mainly leading to an abatement of the relative EDC and a limited decrease of the relative UV_{254} (Fig. 1c, Table S1). In phase II (> 50% EDC abatement), the oxidation of less reactive NOM moieties led to aromatic ring cleavage, resulting in larger UV_{254} abatements (Fig. 1c, Table S1) (Chen et al. 2016, Gordon et al. 1972, Li et al. 2008).

3.2.2. EDC and UV_{254} abatement by O_3 with and without t-BuOH.

Compared to the other oxidants, O_3 led to lower relative EDC and higher relative UV_{254} abatements (Figs. 1a and 1b). The main mechanisms for the O_3 reactions are oxygen transfer (two-electron abstraction) and electron transfer (one-electron transfer) (von Sonntag and von Gunten 2012). For electron transfer, the secondary oxidant $^{\bullet}OH$ is formed, which needs to be taken into consideration during ozonation (de Vera et al. 2015, von Sonntag and von Gunten 2012). $^{\bullet}OH$ can further react with NOM, by hydroxylation or H atom abstraction (von Sonntag 2007), or can catalyze O_3 decomposition (von Sonntag and von Gunten 2012). To evaluate the impact of $^{\bullet}OH$ on NOM properties, *t*-BuOH was added as a scavenger. Similar UV_{254} abatements were obtained with or without *t*-BuOH (Fig. 1b), while the EDC was significantly more abated in presence of *t*-BuOH (Fig. 1a). The similar UV_{254} abatement observed with or without *t*-BuOH suggests that fast-reacting moieties leading to ring cleavage are not affected by the $^{\bullet}OH$-catalyzed decomposition of O_3 (Fig. 1b). However, in absence of

t-BuOH, the lower O_3 exposure (due to $^{\bullet}OH$-catalyzed decomposition), leaded to a lower EDC abatement (Fig. 1a). Additionally, in absence of *t*-BuOH the hydroxylation of aromatic moieties by $^{\bullet}OH$, which may lead to the formation of electron-donating compounds, can also result in a lower EDC abatement.

Despite the higher relative EDC abatement compared to the UV_{254}, similar to the other oxidants in phase I (Fig. 1c), O_3-*t*-BuOH oxidation led to a lower relative $\Delta EDC/\Delta UV_{254}$ abatement ratio ($\Delta EDC/\Delta UV_{254} \approx 3$ for O_3-*t*-BuOH versus 7–8 for the other oxidants, Table S1). Similarly to ClO_2, the higher EDC abatement compared to UV_{254} obtained with O_3-*t*-BuOH has previously been explained by the formation of quinones (Önnby et al. 2018a). However, while benzoquinone is formed stoichiometrically by oxidation of phenol with ClO_2 (Rougé et al. 2018), multiple products are formed (along with benzoquinone) with O_3-*t*-BuOH (Mvula and von Sonntag 2003, Tentscher et al. 2018). In particular, aliphatic compounds are produced by O_3-*t*-BuOH through a Criegee-type mechanism leading to a cleavage of C=C bonds (Ramseier and von Gunten 2009), which mitigates both EDC and UV_{254} and can explain the lower $\Delta EDC/\Delta UV_{254}$ ratios compared to ClO_2 (Fig. 1c, Table S1).

3.2.3. Impact of in situ formed FAC on EDC and UV_{254} abatements during ClO_2 treatment.

Although ClO_2 is generally described as reacting through one-electron transfer reactions (Gordon et al. 1972), oxygen transfer with radical intermediates can also occur, corresponding to a three-electron transfer releasing FAC (Rougé et al. 2018). The *in situ* formed FAC can further react, increasing the oxidation capacity of ClO_2 and potentially the relative EDC abatement. The impact of FAC on the EDC abatement was tested by quenching the *in situ* formed FAC with NH_4Cl, forming NH_2Cl which is significantly less reactive with NOM than FAC (Deborde and von Gunten 2008, Heeb et al. 2017). It was shown that quenching FAC was not or only slightly impacting the EDC abatement whereas it significantly inhibited the UV_{254} abatement (see details in Text S4 and Fig. S2 in SI). The

impact of FAC on UV_{254} but not on EDC suggests that FAC doesn't react with electron-donating compounds, probably because they are already abated by ClO_2, or if FAC reacts, electron-donating compounds may still lead to EDC (e.g., chlorophenols). However, FAC could react with chromophoric compounds that have little reactivity with ClO_2. For instance, FAC can react with quinone-type structures by electrophilic substitution (Zhao et al. 2012). In this case the EDC won't be affected, as quinone-type structures are already oxidized, while the UV_{254} may decrease. The halogenation of quinones can reduce their UV-absorbing properties at 254 nm. As an example, 1,4-benzoquinone has a $\varepsilon_{254} \approx 1.6 \times 10^4$ M^{-1} cm^{-1} whereas for 2,6-dichloro-1,4-benzoquinone and 2,3,6-trichloro-1,4-benzoquinone $\varepsilon_{254} \approx 4 \times 10^3$ M^{-1} cm^{-1} (Qian et al. 2013, Wilke et al. 2013). Multi-halogenation of quinones can also lead to ring cleavage (Rook 1977), which would significantly mitigate their UV_{254}. Halogenation of NOM by *in situ* produced FAC during ClO_2 treatment has previously been demonstrated (Rougé et al. 2018).

3.3. Correlation of chlorine demand and DBP formation with NOM characteristics.

The impact of pre-oxidation on DBP formation and FAC demand are presented in Figs. 2a-h. In practice, other treatments, coagulation/sedimentation or (bio)filtration, may be applied between pre-oxidation and disinfection, which would also affect NOM properties as well as the formation of DBPs (Krasner 2009). Therefore, the correlations presented below solely discuss NOM transformations induced by pre-oxidation and are likely to differ in a more realistic water treatment scheme.

3.3.1. Correlations of NOM characteristics with FAC demand and AOX formation.

Experiments carried out with solutions containing 3 mgC L^{-1} of SRNOM at pH 8, a chlorine dose of 85 µM (6.0 $mgCl_2$ L^{-1}), without or with bromide (150 µg L^{-1}) and without pre-oxidation treatment showed that 58 ± 2 µM of FAC was consumed (Figs. 2a-b) while

16 ± 0.4 µM of AOX was produced after 72 h (Figs. 2c-d). The presence of bromide was not significantly impacting the FAC demand over 72 h. Similarly, the total molar AOX formation was not affected by the presence of bromide, however, part of the chlorine was most likely substituted by bromine in NOM (Langsa et al. 2017b).

The FAC demand after 72 h was decreasing with increasing pre-oxidant doses and the different oxidants exhibited different patterns (Fig. S3a, SI). For example, specific pre-oxidant doses of 2, 5, 7 and 17 µM ox mgC^{-1} were needed to reduce the FAC demand by ~ 20% for Mn(VII), ClO_2, O_3-*t*-BuOH and Fe(VI), respectively. The formation of H_2O_2 during O_3-*t*-BuOH pre-treatment (Acero and Gunten 2000, Tentscher et al. 2018), is suspected to be responsible for a significant fraction of the FAC demand (see details in Text S5, SI) (Held et al. 1978). Therefore, a FAC demand corrected for the impact of H_2O_2 is also presented in Figs. 2a-b and Fig. S3a (SI) (open circles) and is used for the discussion. H_2O_2 is also formed during Fe(VI) decomposition, but it is quickly degraded by Fe(III), Fe(IV) and Fe(V) in absence of phosphate (Jiang et al. 2016a, Lee et al. 2014). The AOX formation after 72 h chlorination also varied depending on the pre-oxidant (Fig. S3b, SI). To achieve a ~ 20% reduction in AOX, specific pre-oxidant doses of 2–3 µM ox mgC^{-1} for O_3-*t*-BuOH or Mn(VII) and 13 and 17 µM ox mgC^{-1} for ClO_2 and Fe(VI) were needed, respectively. Figs. 2a-b and 2c-d show the FAC demand and the AOX formation compared to the relative UV_{254} and EDC abatement for the different oxidants, respectively.

The FAC demand was poorly correlated to the relative UV_{254} abatement (Fig. 2a). The correlation factor was driven by the O_3-*t*-BuOH data corrected for the H_2O_2/FAC reaction (R^2 = 0.840 and 0.693 with and without the corrected O_3-*t*-BuOH data, respectively, Fig. 2a). In comparison, a two-step correlation was observed between the FAC demand and the relative EDC abatement for ClO_2, Fe(VI) and Mn(VII) (Fig. 2b). In the first step, < 50% EDC abatement, the FAC demand was not significantly reduced. In the second step, > 50% EDC

abatement, the FAC demand was significantly reduced and correlated to the relative EDC abatement (R^2 = 0.772, Fig. 2b). Compared to other oxidants (ClO_2, Fe(VI), and Mn(VII)), the O_3-*t*-BuOH (corrected for H_2O_2/FAC reaction) exhibited a higher FAC demand abatement relative to the % EDC abatement (Fig. 2b).

The AOX formation for ClO_2, Fe(VI) and Mn(VII), relative to the % EDC abatement also exhibited a two-step correlation (Fig. 2d). The AOX formation was poorly abated in the first step (< 50% EDC abatement) and significantly abated in the second step (> 50% EDC abatement). The AOX formation after pre-oxidation with ClO_2, Fe(VI) and Mn(VII) had a good correlation with the relative EDC abatement (R^2 = 0.938 in phase II, Fig. 2d) and the relative UV_{254} abatement, although the correlation with the latter was driven by O_3-*t*-BuOH data (R^2 = 0.902 and 0.770 with and without the O_3-*t*-BuOH data, respectively, Fig. 2c). The reduction of AOX formation as a function of the relative EDC abatement was more efficient after O_3-*t*-BuOH pre-oxidation compared to the other oxidants in both phases (Fig. 2d). It has to be noted that the lower FAC exposure induced by the presence of H_2O_2 after O_3-*t*-BuOH pre-oxidation doesn't significantly affect the AOX formation since FAC was always in excess and the chlorination experiments were run over 72 h.

The two-phase trend between the FAC demand, or the AOX formation, and the EDC abatement are explained based on the mechanisms previously described. In phase I, ClO_2, Mn(VII) and Fe(VI) mainly oxidized highly reactive phenolic-type moieties to quinone-type moieties. These moieties have a lower EDC, but can still react with chlorine (Zhao et al. 2012). Therefore, a limited reduction in FAC demand was observed (< 10%) at low relative EDC abatement (≤50%, Fig. 2b). Due to the limited reduction in FAC demand, the AOX formation was not significantly reduced (< 10%, Fig. 2d). In phase II, less-reactive aromatic moieties were cleaved to aliphatic-type moieties. These aliphatic-type moieties are likely to be less readily chlorinated than the original aromatic moieties (Dickenson et al. 2008).

Therefore, the FAC demand (Fig. 2b) and consequently the AOX formation (Fig. 2d) were greatly decreased. For O_3-*t*-BuOH, UV_{254} was significantly abated for low relative EDC abatements (< 50%) (Fig. 1c). Therefore, the availability of reactive aromatic moieties was reduced and led to lower AOX formation and FAC demand (when corrected for H_2O_2/FAC reaction, see details in Text S5, SI) compared to the other oxidants (Figs. 2b and 2d).

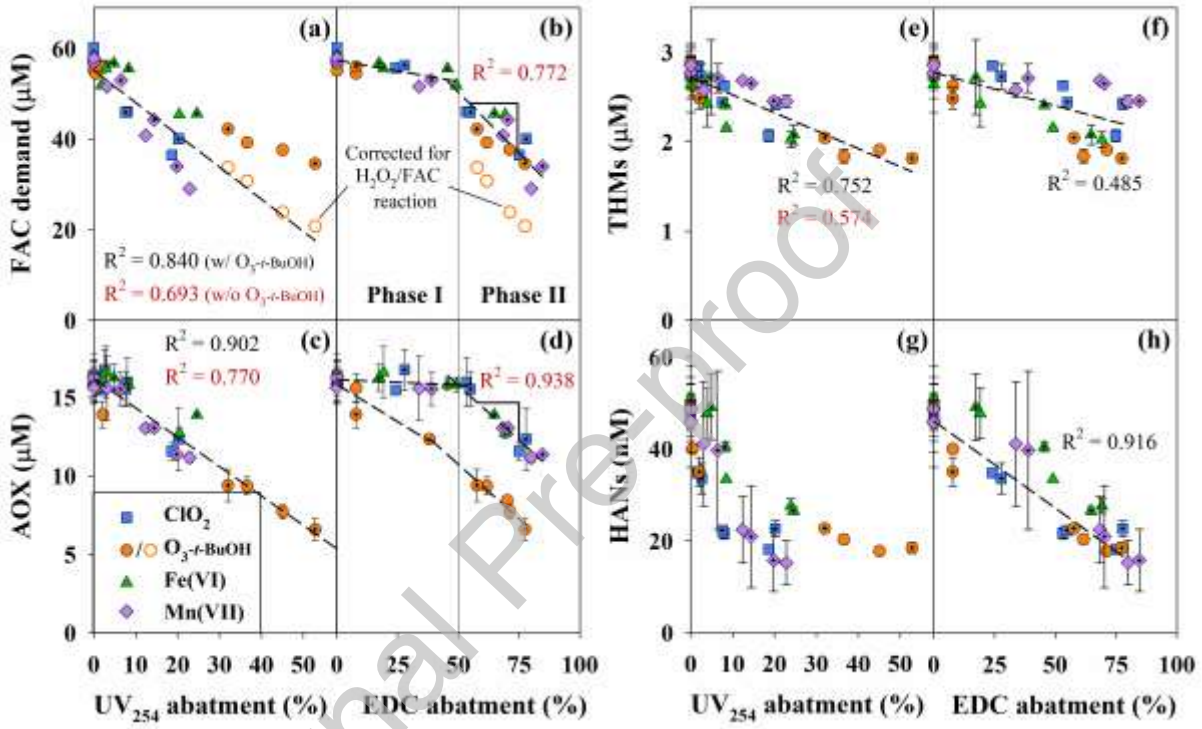

Fig. 2. (a-b) FAC demand and the formation of (c-d) AOX, (e-f) THM and (g-h) HAN as a function of the relative UV_{254} and the relative EDC abatement, respectively. For O_3-*t*-BuOH pre-treatment, the FAC demand was corrected for the H_2O_2 produced in this process (open circles, see Text S5, SI). Black and red correlation factors (p-value < 0.0001) include and exclude O_3-*t*-BuOH data (corrected for H_2O_2/FAC reaction in Fig. 2a), respectively. Linear regressions were done on 32 samples in Figs. a, c, f and h (24 without O_3-*t*-BuOH data) and on 12 samples in Figs b and d. Samples containing bromide are identified by a cross in the symbol. [SRNOM] = 3 mgC L^{-1}, [Br^-] = 0 or 150 µg L^{-1}, 40 mM borate (pH 8), pre-oxidant doses: ClO_2 = 1.2–13 µM mgC^{-1}, O_3-*t*-BuOH = 0.7–31 µM mgC^{-1} ([*t*-BuOH] = 0.4 mM), Fe(VI) = 0.8–17 µM mgC^{-1}, Mn(VII) = 0.3–6.6 µM mgC^{-1}; post-chlorination: FAC dose = 85

µM, 72 h. The data points for DBP formation represent the average of duplicate or triplicate experiments and the error bars the range of obtained data (the two highest doses of Fe(VI) and Mn(VII) were not duplicate experiments).

3.3.2. Correlations of NOM characteristics with THM and HAN formation.

The impact of pre-oxidation on THM and HAN formation was also evaluated. THMs are important regulated DBPs (USEPA 1998), and HANs are unregulated but highly toxic (Muellner et al. 2007). Chlorination experiments (85 µM, 6.0 mgCl_2 L^{-1}) carried out with solutions containing 3 mgC L^{-1} of SRNOM at pH 8, with or without bromide (150 µg L^{-1}) and without pre-oxidation treatment showed that 2.8 ± 0.1 µM of THMs (Figs. 2e-f) and 48 ± 2 nM of HANs (Figs. 2g-h) were formed after 72 h. The presence of bromide did not affect the total formation of THMs and HANs even though brominated DBPs were formed.

As observed for AOX and FAC demand, the correlation between the THM formation and UV_{254} was largely driven by the O_3-*t*-BuOH data (R^2 = 0.752 and 0.574 with and without the O_3-*t*-BuOH data, respectively, Fig. 2e). Overall, the THM formation was poorly correlated to both the relative abatements of UV_{254} (R^2 = 0.574 for THMs/UV_{254}, Fig. 2e) and EDC (R^2 = 0.485 for THMs/EDC, Fig. 2f). The THMs/EDC correlation for O_3-*t*-BuOH pre-treatment was in agreement with a previous study conducted under different experimental conditions (Fig. S5b, SI) (Önnby et al. 2018a). These results suggest that, even though correlations between THM formation and UV_{254} have already been shown in several previous studies (Amy et al. 1987, Edzwald et al. 1985), neither UV_{254} nor EDC were found to be good pre-oxidant-independent THM precursor surrogates.

The formation of HANs was not correlated to the dose of oxidants (Fig. S3d, SI) or the relative UV_{254} abatement (Fig. 2g), which is consistent with a previous study (Hua et al. 2015). Conversely, a good correlation was found with the relative EDC abatement

(R^2 = 0.916, Fig. 2h). HAN formation has been extensively studied, and primary amines are suggested as main precursors (Shah and Mitch 2012). Table S3 summarizes published second order rate constants for the reactions of ClO_2, O_3, Mn(VII) and Fe(VI) with phenol and some amino acids. Aliphatic amino acids such as alanine or aspartic acid are commonly found in water (Dotson and Westerhoff 2009), and can produce HANs upon chlorination (Bond et al. 2009, Bond et al. 2014). However, these amino acids are unreactive with $ABTS^{+\bullet}$ and will hence not contribute to the EDC (Zheng et al. 2016). More importantly, although O_3-*t*-BuOH and Fe(VI) exhibit some reactivity with aliphatic amino acids (apparent second order rate constants of 10^2–10^3 M^{-1} s^{-1} and 10^1–10^2 M^{-1} s^{-1}, respectively, at pH 8) (Hoigné and Bader 1983, Noorhasan et al. 2010, Pryor et al. 1984), Mn(VII) (apparent second order rate constants ≤ 10^{-3} M^{-1} s^{-1} at pH 8) (de Andres et al. 1988, Perez-Benito 2009) and ClO_2 (apparent second order rate constants ≤ 10^{-2} M^{-1} s^{-1} at pH 8) (Hoigné and Bader 1994, Noss et al. 1986) are essentially unreactive with these compounds. Therefore, since a similar HAN mitigation was observed for all the oxidants (Fig. 2h), other precursors might be responsible for HAN formation.

Aromatic amino acids such as tryptophan and tyrosine, commonly used to characterize NOM by fluorescence (Coble et al. 1990), are accounted for in the EDC (Zheng et al. 2016), and yield to significant HAN formation from chlorination (Bond et al. 2009, Jia et al. 2016). The correlation between HAN formation and EDC abatement may be explained by the reactivity of the pre-oxidants with HAN precursors, namely, aromatic amino acids. At pH 8, tryptophan, tyrosine and phenol react with second order rate constants of a similar order of magnitude with O_3 (10^6–10^7 M^{-1} s^{-1} at pH 8), and ClO_2 (10^5–10^6 M^{-1} s^{-1} at pH 8) (Hoigné and Bader 1983, 1994, Pryor et al. 1984, Stewart et al. 2008) (Table S3). Similarly, Fe(VI) oxidizes tryptophan and phenol with similar second order rate constants (10^1–10^2 M^{-1} s^{-1} at pH 8) (Casbeer et al. 2013, Lee et al. 2005a) (Table S3). No data is available for the second

order rate constants for the reaction of tryptophan or tyrosine with Mn(VII), but rough estimations from literature indicate apparent second order rate constants of < 5 M^{-1} s^{-1} (almost no reaction observed) and 10^2 M^{-1} s^{-1}, respectively, at pH 7.2 (Kim et al. 2018). These second order rate constants are within an order of magnitude of the reaction of Mn(VII) with phenol (7–45 M^{-1} s^{-1} at pH 7–8) (Du et al. 2012). Overall, tryptophan-like or tyrosine-like moieties will degrade to an extent similar to phenolic moieties with all the different pre-oxidants, and their degradation should be correlated to the EDC abatement (more kinetic data are needed to be conclusive for Mn(VII)). This may explain the concomitant abatement of EDC (through the degradation of phenolic compounds) and HAN mitigation (through the abatement of tryptophan-like or tyrosine-like precursors).

The results presented in Fig. 2h suggest that aliphatic amino acids, may not be the primary HAN precursors in the examined system. Furthermore, the mitigation of HAN formation may occur through the degradation of a side chain (e.g., indole or phenol group in tryptophan and tyrosine, respectively) rather than direct reaction with the primary amine since ClO_2 and Mn(VII) have low reactivities with primary amines. For example, ClO_2 and O_3 have been shown to oxidize the phenolic side-chain of tyrosine, leading to the formation of a quinone followed by spontaneous cyclization between the primary amine and the quinone, i.e. the formation of dopachrome (Napolitano et al. 2005, Verweij et al. 1982). Although the chlorination of dopachrome is unknown, it can be hypothesized that the HAN yield from this compound will be lower compared to the tyrosine. N-containing structures other than amino acids may produce HANs (Ueno et al. 1996, Yang et al. 2012), but are not discussed here due to a lack of literature on their reactivities with oxidants.

3.3.3. Correlations of NOM characteristics with calculated toxicity.

The total relative cytotoxicity has previously been used as a tool to assess the adverse effects induced by the formation of DBPs and compare different treatment options (Allard et al.

2015, Ersan et al. 2019, Smith et al. 2010). The total relative cytotoxicity is calculated as the sum of the ratios between the concentration of a specific DBP (C) and its cytotoxicity (C_{50}) (eq 1). The cytotoxicity is represented by the concentration of a specific DBP resulting in a 50% reduction of Chinese hamster ovary cells density after 72 h (Plewa et al. 2008).

$$Total\ relative\ cytoxicity = \sum \frac{C}{C_{50}} \qquad (1)$$

Although the THM concentration was about 50 times higher than the HAN concentration (Figs. 2e-h), the cytotoxicity of HANs is several orders of magnitude higher (C_{50} = 10^{-3}–10^{-2} and 10^{-6}–10^{-4} M for THMs and HANs, respectively, see Tables S4, SI) (Plewa et al. 2008). Therefore, under our experimental conditions, THM-induced cytotoxicity was much lower than HAN-induced toxicity, as illustrated in Fig. 3. Even though only two DBP classes were monitored, the importance of HAN-induced toxicity is consistent with previous studies (Plewa et al., 2017, Ersan et al. 2019).

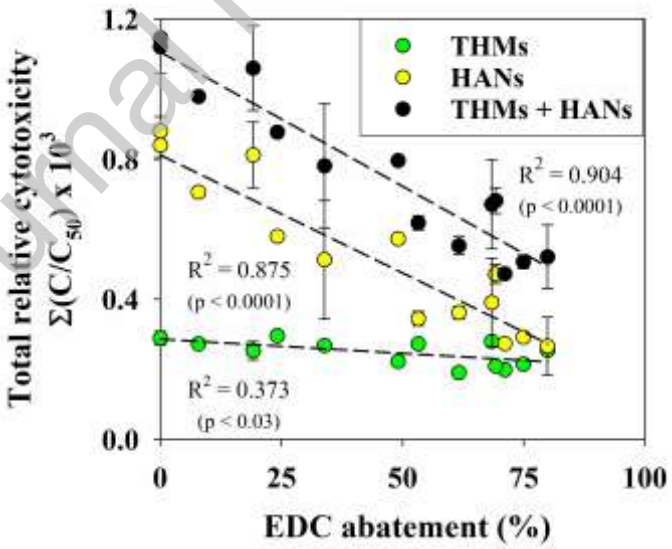

Fig. 3. Calculated cytotoxicity as a function of the EDC abatement. For each linear regression, the number of samples was 16. [SRNOM] = 3 mgC L^{-1}, 40 mM borate (pH 8), no Br^-, pre-oxidant doses: ClO_2 = 1.2–13 µM mgC^{-1}, O_3-*t*-BuOH = 0.7–31 µM mgC^{-1} ([*t*-BuOH] = 0.4 mM), Fe(VI) = 0.8–17 µM mgC^{-1}, Mn(VII) = 0.3–6.6 µM mgC^{-1}; post-chlorination:

FAC dose = 85 µM, 72 h. The data used for the cytotoxicity calculations are provided in Tables S4 and S5 (SI).

The good correlation observed between EDC abatement and HAN formation (Fig. 2h) translated, in absence of bromide, to a good correlation between EDC abatement and calculated cytotoxicity (R^2 = 0.904, Fig. 3). Conversely, the poor correlation between UV_{254} abatement and HAN formation led to a poor correlation between UV_{254} abatement and calculated cytotoxicity (R^2 = 0.637, Fig. S6, SI). In presence of 150 µg L^{-1} bromide, the calculated total relative cytotoxicity was not correlated with the EDC abatement (R^2 = 0.262, Fig. S7b, SI), due to the very potent brominated HANs which were less efficiently mitigated (see Table S6, SI). Alternatively, a total relative genotoxicity, representing DBP-induced DNA damage, can be calculated (see details in Text S6 and Fig. S8, SI) (Muellner et al. 2007). As observed for cytotoxicity, THMs were not relevant (they don't lead to quantifiable DNA damage) (Plewa et al. 2008) while bromide highly affected genotoxicity and led to a poor correlation with EDC abatement (Fig. S8, SI). Other DBPs such as haloacetamides, halonitromethanes or haloaldehydes exhibit significant cytotoxicity and genotoxicity (Wagner and Plewa 2007, Plewa et al. 2017), and could strongly impact the correlation observed between EDC abatement and calculated toxicity. Therefore, monitoring these DBPs, or performing toxicity assays, is essential to better assess the suitability of UV_{254} and EDC as surrogates for pre-treatment efficiency related to toxicity.

4. Conclusions

An efficient control of the pre-oxidant dose is a prerequisite for an optimized disinfectant demand, to mitigate the formation of potentially toxic DBPs while maintaining a disinfectant residual. For pre-oxidation with ClO_2, Mn(VII) or Fe(VI), a minimum EDC abatement (50% under our experimental conditions) is required to abate FAC-reactive moieties efficiently.

Compared to the EDC, the relative UV_{254} abatement occurs to a much lower extent, which leads to a significantly smaller measurement range and hence accuracy problems. This is especially important for low pre-oxidant doses and can be amplified by interferences from UV-absorbing compounds commonly found in natural or treated waters such as nitrate, chlorite or metals (Weishaar et al. 2003). These inaccuracies can lead to an overdosing of FAC, resulting in the formation of higher concentrations of DBPs. To address the growing concern about potent DBPs, additional emerging DBPs will probably be regulated. Although UV_{254} has been shown to be a good surrogate for AOX, it is poorly correlated to emerging DBPs (Hua et al. 2015). The correlation observed between HAN formation and EDC abatement is promising and EDC should be further explored as a surrogate for the formation of emerging DBPs. To mimic more realistic water treatment conditions, the impact of real water matrices and of all treatment steps between pre-oxidation and chlorination on NOM reactivity, notably biofiltration, needs to be investigated. Overall, EDC and UV_{254} can be used to determine the degree of oxidative pre-treatment and the required disinfectant dose to achieve optimal water treatment, hence minimizing the DBP-induced toxicity.

Acknowledgments

We acknowledge Peter Hopper for his assistance with GC-MS. Curtin University (Curtin International postgraduate Research Scholarship) and Curtin Water Quality Research Centre are also acknowledged for providing financial support for V.R.

Appendix A. Supplementary data

Supplementary data related to this article can be found at:

ORCID

Valentin Rougé: 0000-0002-6452-2209

Urs von Gunten: 0000-0001-6852-8977

Sébastien Allard: 0000-0002-6937-4671

Notes

The authors declare no competing financial interest.

Declaration of interests

☒ The authors declare that they have no known competing financial interests or personal relationships that could have appeared to influence the work reported in this paper.

☐The authors declare the following financial interests/personal relationships which may be considered as potential competing interests:

REFERENCES

Acero, J.L. and Gunten, U.v. (2000) Influence of Carbonate on the Ozone/Hydrogen Peroxide Based Advanced Oxidation Process for Drinking Water Treatment. Ozone-Sci. Eng. 22(3), 305-328.

Aeschbacher, M., Graf, C., Schwarzenbach, R.P. and Sander, M. (2012) Antioxidant properties of humic substances. Environ. Sci. Technol. 46(9), 4916-4925.

Allard, S., Charrois, J.W.A., Joll, C.A. and Heitz, A. (2012) Simultaneous analysis of 10 trihalomethanes at nanogram per liter levels in water using solid-phase microextraction and gas chromatography mass-spectrometry. J. Chromatogr. A 1238, 15-21.

Allard, S., Gutierrez, L., Fontaine, C., Croué, J.-P. and Gallard, H. (2017) Organic matter interactions with natural manganese oxide and synthetic birnessite. Sci. Total Environ. 583, 487-495.

Allard, S., Tan, J., Joll, C.A. and von Gunten, U. (2015) Mechanistic Study on the Formation of Cl-/Br-/I-Trihalomethanes during Chlorination/Chloramination Combined with a Theoretical Cytotoxicity Evaluation. Environ. Sci. Technol. 49(18), 11105-11114.

Amy, G.L., Chadik, P.A. and Chowdhury, Z.K. (1987) Developing Models for Predicting Trihalomethane Formation Potential and Kinetics. J. Am. Water Works Ass. 79(7), 89-97.

Archer, A.D. and Singer, P.C. (2006) Effect of SUVA and enhanced coagulation on removal of TOX precursors. J. Am. Water Works Ass. 98(8), 97-107.

Ates, N., Kitis, M. and Yetis, U. (2007) Formation of chlorination by-products in waters with low SUVA—correlations with SUVA and differential UV spectroscopy. Water Res. 41(18), 4139-4148.

Bond, T., Henriet, O., Goslan, E.H., Parsons, S.A. and Jefferson, B. (2009) Disinfection Byproduct Formation and Fractionation Behavior of Natural Organic Matter Surrogates. Environ. Sci. Technol. 43(15), 5982-5989.

Bond, T., Mokhtar Kamal, N.H., Bonnisseau, T. and Templeton, M.R. (2014) Disinfection by-product formation from the chlorination and chloramination of amines. J. Hazard. Mater. 278, 288-296.

Casbeer, E.M., Sharma, V.K., Zajickova, Z. and Dionysiou, D.D. (2013) Kinetics and Mechanism of Oxidation of Tryptophan by Ferrate(VI). Environ. Sci. Technol. 47(9), 4572-4580.

Chen, J., Qu, R., Pan, X. and Wang, Z. (2016) Oxidative degradation of triclosan by potassium permanganate: Kinetics, degradation products, reaction mechanism, and toxicity evaluation. Water Res. 103, 215-223.

Chen, Z. and Valentine, R.L. (2008) The influence of the pre-oxidation of natural organic matter on the formation of N-nitrosodimethylamine (NDMA). Environ. Sci. Technol. 42(14), 5062-5067.

Chon, K., Salhi, E. and von Gunten, U. (2015) Combination of UV absorbance and electron donating capacity to assess degradation of micropollutants and formation of bromate during ozonation of wastewater effluents. Water Res. 81, 388-397.

Coble, P.G., Green, S.A., Blough, N.V. and Gagosian, R.B. (1990) Characterization of dissolved organic matter in the Black Sea by fluorescence spectroscopy. Nature 348, 432.

Criquet, J., Rodriguez, E.M., Allard, S., Wellauer, S., Salhi, E., Joll, C.A. and von Gunten, U. (2015) Reaction of bromine and chlorine with phenolic compounds and natural organic matter extracts - Electrophilic aromatic substitution and oxidation. Water Res. 85, 476-486.

Croué, J.-P., Violleau, D. and Labouyrie, L. (2000) Natural Organic Matter and Disinfection By-Products, pp. 139-153, American Chemical Society.

de Andres, J., Brillas, E., Garrido, J.A. and Perez-Benito, J.F. (1988) Kinetics and mechanisms of the oxidation by permanganate of L-alanine. J. Chem. Soc. Perkin Trans. 2 (2), 107-112.

de Vera, G.A., Stalter, D., Gernjak, W., Weinberg, H.S., Keller, J. and Farré, M.J. (2015) Towards reducing DBP formation potential of drinking water by favouring direct ozone over hydroxyl radical reactions during ozonation. Water Res. 87, 49-58.

de Vera, G.A., Gernjak, W. and Radjenovic, J. (2017) Predicting reactivity of model DOM compounds towards chlorine with mediated electrochemical oxidation. Water Res. 114, 113-121.

Deborde, M. and von Gunten, U. (2008) Reactions of chlorine with inorganic and organic compounds during water treatment—Kinetics and mechanisms: A critical review. Water Res. 42(1–2), 13-51.

Dickenson, E.R.V., Summers, R.S., Croué, J.-P. and Gallard, H. (2008) Haloacetic acid and Trihalomethane Formation from the Chlorination and Bromination of Aliphatic β-Dicarbonyl Acid Model Compounds. Environ. Sci. Technol. 42(9), 3226-3233.

Dotson, A. and Westerhoff, P. (2009) Occurrence and removal of amino acids during drinking water treatment. J. Am. Water Works Ass. 101(9), 101-115.

Du, J., Sun, B., Zhang, J. and Guan, X. (2012) Parabola-Like Shaped pH-Rate Profile for Phenols Oxidation by Aqueous Permanganate. Environ. Sci. Technol. 46(16), 8860-8867.

Edzwald, J.K., Becker, W.C. and Wattier, K.L. (1985) Surrogate Parameters for Monitoring Organic Matter and THM Precursors. J. Am. Water Works Ass. 77(4), 122-132.

Ersan, M.S., Liu, C., Amy, G. and Karanfil, T. (2019) The interplay between natural organic matter and bromide on bromine substitution. Sci. Total Environ. 646, 1172-1181.

Furman, C.S. and Margerum, D.W. (1998) Mechanism of Chlorine Dioxide and Chlorate Ion Formation from the Reaction of Hypobromous Acid and Chlorite Ion. Inorg. Chem. 37(17), 4321-4327.

Gallard, H. and von Gunten, U. (2002) Chlorination of natural organic matter: kinetics of chlorination and of THM formation. Water Res. 36(1), 65-74.

Gan, W., Sharma, V.K., Zhang, X., Yang, L. and Yang, X. (2015) Investigation of disinfection byproducts formation in ferrate(VI) pre-oxidation of NOM and its model compounds followed by chlorination. J. Hazard. Mater. 292, 197-204.

Gates, D.J. (1998) The Chlorine Dioxide Handbook, American Water Works Association.

Gordon, G., Kieffer, R.G. and Rosenblatt, D.H. (1972) Progress in Inorganic Chemistry. Lippard, S.J. (ed), pp. 201-286, John Wiley & Sons, Inc., New York.

Granstrom, M.L. and Lee, G.F. (1958) Generation and Use of Chlorine Dioxide in Water Treatment. J. Am. Water Works Ass. 50(11), 1453-1466.

Heeb, M.B., Kristiana, I., Trogolo, D., Arey, J.S. and von Gunten, U. (2017) Formation and reactivity of inorganic and organic chloramines and bromamines during oxidative water treatment. Water Res. 110(Supplement C), 91-101.

Held, A.M., Halko, D.J. and Hurst, J.K. (1978) Mechanisms of chlorine oxidation of hydrogen peroxide. J. Am. Chem. Soc. 100(18), 5732-5740.

Helms, J.R., Stubbins, A., Ritchie, J.D., Minor, E.C., Kieber, D.J. and Mopper, K. (2008) Absorption spectral slopes and slope ratios as indicators of molecular weight, source, and photobleaching of chromophoric dissolved organic matter. Limnol. Oceanogr. 53(3), 955-969.

Hoigné, J. and Bader, H. (1983) Rate constants of reactions of ozone with organic and inorganic compounds in water—II. Water Res. 17(2), 185-194.

Hoigné, J. and Bader, H. (1994) Kinetics of reactions of chlorine dioxide (OClO) in water-I. Rate constants for inorganic and organic compounds. Water Res. 28(1), 45-55.

Hua, G., Reckhow, D.A. and Abusallout, I. (2015) Correlation between SUVA and DBP formation during chlorination and chloramination of NOM fractions from different sources. Chemosphere 130, 82-89.

Huang, H., Sommerfeld, D., Dunn, B.C., Eyring, E.M. and Lloyd, C.R. (2001) Ferrate(VI) Oxidation of Aqueous Phenol: Kinetics and Mechanism. J. Phys. Chem. A 105(14), 3536-3541.

Jia, A., Wu, C. and Duan, Y. (2016) Precursors and factors affecting formation of haloacetonitriles and chloropicrin during chlor(am)ination of nitrogenous organic compounds in drinking water. J. Hazard. Mater. 308, 411-418.

Jiang, J., Pang, S.-Y. and Ma, J. (2009) Oxidation of Triclosan by Permanganate (Mn(VII)): Importance of Ligands and In Situ Formed Manganese Oxides. Environ. Sci. Technol. 43(21), 8326-8331.

Jiang, J., Pang, S.-Y., Ma, J. and Liu, H. (2012) Oxidation of Phenolic Endocrine Disrupting Chemicals by Potassium Permanganate in Synthetic and Real Waters. Environ. Sci. Technol. 46(3), 1774-1781.

Jiang, Y., Goodwill, J.E., Tobiason, J.E. and Reckhow, D.A. (2016a) Bromide oxidation by ferrate(VI): The formation of active bromine and bromate. Water Res. 96, 188-197.

Jiang, Y., Goodwill, J.E., Tobiason, J.E. and Reckhow, D.A. (2016b) Ferrites and Ferrates: Chemistry and Applications in Sustainable Energy and Environmental Remediation, pp. 421-437, American Chemical Society.

Jiang, Y., Goodwill, J.E., Tobiason, J.E. and Reckhow, D.A. (2016c) Impacts of ferrate oxidation on natural organic matter and disinfection byproduct precursors. Water Res. 96, 114-125.

Jones, D.B., Song, H. and Karanfil, T. (2012) The effects of selected preoxidation strategies on I-THM formation and speciation. Water Res. 46(17), 5491-5498.

Kim, M.S., Lee, H.-J., Lee, K.-M., Seo, J. and Lee, C. (2018) Oxidation of Microcystins by Permanganate: pH and Temperature-Dependent Kinetics, Effect of DOM Characteristics, and Oxidation Mechanism Revisited. Environ. Sci. Technol. 52(12), 7054-7063.

Korshin, G.V., Li, C.-W. and Benjamin, M.M. (1996) Water Disinfection and Natural Organic Matter, pp. 182-195, American Chemical Society.

Korshin, G.V., Li, C.-W. and Benjamin, M.M. (1997a) The decrease of UV absorbance as an indicator of TOX formation. Water Res. 31(4), 946-949.

Korshin, G.V., Li, C.-W. and Benjamin, M.M. (1997b) Monitoring the properties of natural organic matter through UV spectroscopy: A consistent theory. Water Res. 31(7), 1787-1795.

Korshin, G.V., Wu, W.W., Benjamin, M.M. and Hemingway, O. (2002) Correlations between differential absorbance and the formation of individual DBPs. Water Res. 36(13), 3273-3282.

Krasner, S.W. (2009) The formation and control of emerging disinfection by-products of health concern. Philos. Trans. R. Soc. A. 367(1904), 4077-4095.

Kristiana, I., Joll, C. and Heitz, A. (2012) Analysis of halonitriles in drinking water using solid-phase microextraction and gas chromatography–mass spectrometry. J. Chromatogr. A 1225, 45-54.

Kumar, K. and Margerum, D.W. (1987) Kinetics and mechanism of general-acid-assisted oxidation of bromide by hypochlorite and hypochlorous acid. Inorg. Chem. 26(16), 2706-2711.

Langsa, M., Allard, S., Kristiana, I., Heitz, A. and Joll, C.A. (2017a) Halogen-specific total organic halogen analysis: Assessment by recovery of total bromine. J. Env. Sci. 58, 340-348.

Langsa, M., Heitz, A., Joll, C.A., von Gunten, U. and Allard, S. (2017b) Mechanistic Aspects of the Formation of Adsorbable Organic Bromine during Chlorination of Bromide-containing Synthetic Waters. Environ. Sci. Technol. 51(9), 5146-5155.

Lawani, S.A. and Sutter, J.R. (1973) Kinetic studies of permanganate oxidation reactions. IV. Reaction with bromide ion. The Journal of Physical Chemistry 77(12), 1547-1551.

Lee, Y., Kissner, R. and von Gunten, U. (2014) Reaction of ferrate(VI) with ABTS and self-decay of ferrate(VI): Kinetics and mechanisms. Environ. Sci. Technol. 48(9), 5154-5162.

Lee, Y., Yoon, J. and von Gunten, U. (2005a) Kinetics of the Oxidation of Phenols and Phenolic Endocrine Disruptors during Water Treatment with Ferrate (Fe(VI)). Environ. Sci. Technol. 39(22), 8978-8984.

Lee, Y., Yoon, J. and von Gunten, U. (2005b) Spectrophotometric determination of ferrate (Fe(VI)) in water by ABTS. Water Res. 39(10), 1946-1953.

Li, C., Li, X.Z. and Graham, N. (2005) A study of the preparation and reactivity of potassium ferrate. Chemosphere 61(4), 537-543.

Li, C., Li, X.Z., Graham, N. and Gao, N.Y. (2008) The aqueous degradation of bisphenol A and steroid estrogens by ferrate. Water Res. 42(1), 109-120.

Lim, S., McArdell, C.S. and von Gunten, U. (2019) Reactions of aliphatic amines with ozone: Kinetics and mechanisms. Water Res. 157, 514-528.

Muellner, M.G., Wagner, E.D., McCalla, K., Richardson, S.D., Woo, Y.-T. and Plewa, M.J. (2007) Haloacetonitriles vs. Regulated Haloacetic Acids: Are Nitrogen-Containing DBPs More Toxic? Environ. Sci. Technol. 41(2), 645-651.

Mvula, E. and von Sonntag, C. (2003) Ozonolysis of Phenols in Aqueous Solution. Org. Biomol. Chem. 1, 1749-1756.

Napolitano, M.J., Green, B.J., Nicoson, J.S. and Margerum, D.W. (2005) Chlorine Dioxide Oxidations of Tyrosine, N-Acetyltyrosine, and Dopa. Chem. Res. Toxicol. 18(3), 501-508.

Noorhasan, N., Patel, B. and Sharma, V.K. (2010) Ferrate(VI) oxidation of glycine and glycylglycine: Kinetics and products. Water Res. 44(3), 927-935.

Noss, C.I., Hauchman, F.S. and Olivieri, V.P. (1986) Chlorine dioxide reactivity with proteins. Water Res. 20(3), 351-356.

Önnby, L., Salhi, E., McKay, G., Rosario-Ortiz, F.L. and von Gunten, U. (2018a) Ozone and chlorine reactions with dissolved organic matter - Assessment of oxidant-reactive moieties by optical measurements and the electron donating capacities. Water Res. 144, 64-75.

Önnby, L., Walpen, N., Salhi, E., Sander, M. and Von Gunten, U. (2018b) Two analytical approached to quantify the oxidation of dissolved organic matter by chlorine and ozone. Water Res. 144, 677-689.

Perez-Benito, J.F. (2009) Autocatalytic Reaction Pathway on Manganese Dioxide Colloidal Particles in the Permanganate Oxidation of Glycine. J. Phys. Chem. C 113(36), 15982-15991.

Pinkernell, U., Nowack, B., Gallard, H. and Von Gunten, U. (2000) Methods for the photometric determination of reactive bromine and chlorine species with ABTS. Water Res. 34(18), 4343-4350.

Plewa, M.J., Wagner, E.D., Muellner, M.G., Hsu, K.-M. and Richardson, S.D. (2008) Disinfection By-Products in Drinking Water, pp. 36-50, American Chemical Society.

Plewa, M.J., Wagner, E.D. and Richardson, S.D. (2017) TIC-Tox: A preliminary discussion on identifying the forcing agents of DBP-mediated toxicity of disinfected water. J. Env. Sci. 58, 208-216.

Pryor, W.A., Giamalva, D.H. and Church, D.F. (1984) Kinetics of ozonation. 2. Amino acids and model compounds in water and comparisons to rates in nonpolar solvents. J. Am. Chem. Soc. 106(23), 7094-7100.

Qian, Y., Wang, W., Boyd, J.M., Wu, M., Hrudey, S.E. and Li, X.-F. (2013) UV-Induced Transformation of Four Halobenzoquinones in Drinking Water. Environ. Sci. Technol. 47(9), 4426-4433.

Ramseier, M.K. and Gunten, U.v. (2009) Mechanisms of Phenol Ozonation—Kinetics of Formation of Primary and Secondary Reaction Products. Ozone-Sci. Eng. 31(3), 201-215.

Ramseier, M.K., Peter, A., Traber, J. and von Gunten, U. (2011) Formation of assimilable organic carbon during oxidation of natural waters with ozone, chlorine dioxide, chlorine, permanganate, and ferrate. Water Res. 45(5), 2002-2010.

Reckhow, D.A., Singer, P.C. and Malcolm, R.L. (1990) Chlorination of humic materials: byproduct formation and chemical interpretations. Environ. Sci. Technol. 24(11), 1655-1664.

Remucal, C.K., Salhi, E., Walpen, N. and von Gunten, U. (2020) Molecular-Level Transformation of Dissolved Organic Matter during Oxidation by Ozone and Hydroxyl Radical. Environ. Sci. Technol. 54(16), 10351-10360.

Richardson, S.D., Plewa, M.J., Wagner, E.D., Schoeny, R. and DeMarini, D.M. (2007) Occurrence, genotoxicity, and carcinogenicity of regulated and emerging disinfection by-products in drinking water: A review and roadmap for research. Mutat. Res-Rev. Mutat. 636(1–3), 178-242.

Rook, J.J. (1977) Chlorination reactions of fulvic acids in natural waters. Environ. Sci. Technol. 11(5), 478-482.

Rougé, V., Allard, S., Croué, J.-P. and von Gunten, U. (2018) In Situ Formation of Free Chlorine During ClO_2 Treatment: Implications on the Formation of Disinfection Byproducts. Environ. Sci. Technol. 52(22), 13421-13429.

Rush, J.D. and Bielski, B.H.J. (1989) Kinetics of ferrate(V) decay in aqueous solution. A pulse-radiolysis study. Inorg. Chem. 28(21), 3947-3951.

Rush, J.D. and Bielski, B.H.J. (1995) The Oxidation of Amino Acids By Ferrate(V). A Pre-Mix Pulse Radiolysis Study. Free Radical Res. 22(6), 571-579.

Rush, J.D., Cyr, J.E., Zhao, Z. and Bielski, B.H.J. (1995) The Oxidation of Phenol by Ferrate(VI) and Ferrate(V). A Pulse Radiolysis and Stopped-Flow Study. Free Radical Res. 22(4), 349-360.

Sedlak, D.L. and von Gunten, U. (2011) The Chlorine Dilemma. Science 331(6013), 42-43.

Selbes, M., Kim, D. and Karanfil, T. (2014) The effect of pre-oxidation on NDMA formation and the influence of pH. Water Res. 66, 169-179.

Shah, A.D. and Mitch, W.A. (2012) Halonitroalkanes, Halonitriles, Haloamides, and N-Nitrosamines: A Critical Review of Nitrogenous Disinfection Byproduct Formation Pathways. Environ. Sci. Technol. 46(1), 119-131.

Shin, J. and Lee, Y. (2016) Ferrites and Ferrates: Chemistry and Applications in Sustainable Energy and Environmental Remediation, pp. 255-273, American Chemical Society.

Simándi, L. and Záhonyi-Budó, É. (1998) Relative reactivities of hydroxy compounds with short-lived manganese(V). Inorg. Chim. Acta 281(2), 235-238.

Smith, E.M., Plewa, M.J., Lindell, C.L., Richardson, S.D. and Mitch, W.A. (2010) Comparison of Byproduct Formation in Waters Treated with Chlorine and Iodine: Relevance to Point-of-Use Treatment. Environ. Sci. Technol. 44(22), 8446-8452.

Staehelin, J. and Hoigné, J. (1985) Decomposition of ozone in water in the presence of organic solutes acting as promoters and inhibitors of radical chain reactions. Environ. Sci. Technol. 19(12), 1206-1213.

Stewart, D.J., Napolitano, M.J., Bakhmutova-Albert, E.V. and Margerum, D.W. (2008) Kinetics and Mechanisms of Chlorine Dioxide Oxidation of Tryptophan. Inorg. Chem. 47(5), 1639-1647.

Tentscher, P.R., Bourgin, M. and von Gunten, U. (2018) Ozonation of Para-Substituted Phenolic Compounds Yields p-Benzoquinones, Other Cyclic α,β-Unsaturated Ketones, and Substituted Catechols. Environ. Sci. Technol. 52(8), 4763-4773.

Terhalle, J., Kaiser, P., Jütte, M., Buss, J., Yasar, S., Marks, R., Uhlmann, H., Schmidt, T.C. and Lutze, H.V. (2018) Chlorine dioxide – Pollutant transformation and formation of hypochlorous acid as a secondary oxidant. Environ. Sci. Technol 52(17), 9964-9971.

USEPA (1998) Disinfectants and Disinfection Byproducts final rule. 63, 69390-69476.

Ueno, H., Moto, T., Sayato, Y. and Nakamuro, K. (1996) Disinfection by-products in the chlorination of organic nitrogen compounds: By-products from kynurenine. Chemosphere 33(8), 1425-1433.

Verweij, H., Christianse, K. and van Steveninck, J. (1982) Different pathways of tyrosine oxidation by ozone. Chemosphere 11(8), 721-725.

von Gunten, U. (2003) Ozonation of drinking water: Part I. Oxidation kinetics and product formation. Water Res. 37(7), 1443-1467.

von Gunten, U. (2018) Oxidation Processes in Water Treatment: Are We on Track? Environ. Sci. Technol. 52(9), 5062-5075.

von Gunten, U. and Hoigné, J. (1994) Bromate formation during ozonation of bromide-containing waters: Interaction of ozone and hydroxyl radical reactions. Environ. Sci. Technol. 28(7), 1234-1242.

von Sonntag, C. (2007) The basics of oxidants in water treatment. Part A: OH radical reactions. Water Sci. Technol. 55(12), 19-23.

von Sonntag, C. and von Gunten, U. (2012) Chemistry of Ozone in Water and Wastewater Treatment: From Basic Principles to Applications, International Water Association.

Wagner, E.D. and Plewa, M.J. (2017) CHO cell cytotoxicity and genotoxicity analyses of disinfection by-products: An updated review. J. Env. Sci. 58, 64-76.

Waldemer, R.H. and Tratnyek, P.G. (2006) Kinetics of contaminant degradation by permanganate. Environ. Sci. Technol. 40(3), 1055-1061.

Walpen, N., Schroth, M.H. and Sander, M. (2016) Quantification of Phenolic Antioxidant Moieties in Dissolved Organic Matter by Flow-Injection Analysis with Electrochemical Detection. Environ. Sci. Technol. 50(12), 6423-6432.

Walpen, N., Houska, J., Salhi, E., Sander, M. and von Gunten, U. (2020) Quantification of the electron donating capacity and UV absorbance of dissolved organic matter during ozonation of secondary wastewater effluent by an assay and an automated analyzer. Water Res. 185, 116235.

Wang, T. and Reckhow, D.A. (2016) Spectrophotometric Method for Determination of Ozone Residual in Water Using ABTS: 2.2'-Azino-Bis (3-Ethylbenzothiazoline-6-Sulfonate). Ozone-Sci. Eng. 38(5), 373-381.

Weishaar, J.L., Aiken, G.R., Bergamaschi, B.A., Fram, M.S., Fujii, R. and Mopper, K. (2003) Evaluation of Specific Ultraviolet Absorbance as an Indicator of the Chemical Composition and Reactivity of Dissolved Organic Carbon. Environ. Sci. Technol. 37(20), 4702-4708.

Wenk, J., Aeschbacher, M., Salhi, E., Canonica, S., von Gunten, U. and Sander, M. (2013) Chemical oxidation of dissolved organic matter by chlorine dioxide, chlorine, and ozone: Effects on its optical and antioxidant properties. Environ. Sci. Technol. 47(19), 11147-11156.

Wilke, T., Schneider, M. and Kleinermanns, K. (2013) 1,4-Hydroquinone is a Hydrogen Reservoir for Fuel Cells and Recyclable via Photocatalytic Water Splitting. Open J. Phys. Chem. 3, 97-102.

Xie, P., Ma, J., Fang, J., Guan, Y., Yue, S., Li, X. and Chen, L. (2013) Comparison of Permanganate Preoxidation and Preozonation on Algae Containing Water: Cell Integrity, Characteristics, and Chlorinated Disinfection Byproduct Formation. Environ. Sci. Technol. 47(24), 14051-14061.

Yang, X., Shen, Q., Guo, W., Peng, J. and Liang, Y. (2012) Precursors and nitrogen origins of trichloronitromethane and dichloroacetonitrile during chlorination/chloramination. Chemosphere 88(1), 25-32.

Yang, X., Guo, W. and Lee, W. (2013a) Formation of disinfection byproducts upon chlorine dioxide preoxidation followed by chlorination or chloramination of natural organic matter. Chemosphere 91(11), 1477-1485.

Yang, X., Guo, W., Zhang, X., Chen, F., Ye, T. and Liu, W. (2013b) Formation of disinfection by-products after pre-oxidation with chlorine dioxide or ferrate. Water Res. 47(15), 5856-5864.

Záhonyi-Budó, É. and Simándi, L. (1996) Oxidation of propane-1,2-diol by acidic manganese(V) and manganese(VI). Inorg. Chim. Acta 248(1), 81-84.

Zhao, Y., Anichina, J., Lu, X., Bull, R.J., Krasner, S.W., Hrudey, S.E. and Li, X.-F. (2012) Occurrence and formation of chloro- and bromo-benzoquinones during drinking water disinfection. Water Res. 46(14), 4351-4360.

Zheng, L., Zhao, M., Xiao, C., Zhao, Q. and Su, G. (2016) Practical problems when using ABTS assay to assess the radical-scavenging activity of peptides: Importance of controlling reaction pH and time. Food Chem. 192, 288-294.

GRAPHICAL ABSTRACT